Supporting Information

Ogawa et al. 10.1073/pnas.1422203112

SI Methods

Enzyme. Reverse gyrase was purified from *S. tokodaii* as described (1).

DNA Constructs. The bubbled DNA substrates shown in Fig. 1*A* were prepared by annealing a complementary ssDNA pair containing a 30-nt mismatch essentially as described by Hsieh and Plank (2) and appending a biotinylated fragment and a digoxigenin-labeled fragment at each end following the method of Revyakin et al. (3). Details are provided in the legend for Fig. S1.

Observation Chamber. Coverslips were modified with biotinylated PEG for DNA attachment and surface blocking. First, we coated $18 \times 18\text{-mm}^2$ (for chamber top) and $24 \times 32\text{-mm}^2$ (for chamber bottom) coverslips (Matsunami Glass) with (3-mercaptopropyl) trimethoxysilane (Momentive Performance Materials) and reduced the SH groups with DTT basically as described (4). We then sandwiched between pairs of top coverslips 10 mM methyl-PEG-maleimide [molecular weight (MW) of 700; Thermo Scientific] in 50 mM 3-(*N*-morpholino)propanesulfonic acid-NaOH (pH 7.0) and incubated the coverslips overnight at room temperature. The reagent for the chamber bottom contained in addition 0.1 mM biotin-PEG-maleimide (MW of 600; Quanta Bio Design). Finally, we washed the coverslips with water and stored them in water at 4 °C until use.

A flow chamber with a side chamber for a thermocouple (Fig. 1*B*) was made of the modified coverslips separated by three strips of double-sided tape of 80-μm thickness (300A80B; Kyodo Giken Kagaku). We infused one chamber volume (~10 μL) of 1 mg/mL streptavidin (Pierce) in buffer A [10 mM Tris·HCl (pH 7.9), 1 mM EDTA, 50 mM NaCl] into the main chamber, waited for 10 min, and washed out unbound streptavidin with 10 vol of buffer A. Further infusion and incubation were as follows: two chamber volumes of a DNA substrate at ~20 pM in buffer A (5 min); 2 vol of 10 mg/mL biotin-PEG (MW of 5,000; Laysan Bio) in buffer A for blocking unreacted streptavidin on the surface (5 min); 1 vol of carboxylated superparamagnetic beads (1-μm diameter; Dynal) that had been coated with antidigoxigenin antibody (polyclonal; Acris Antibodies) and methyl-PEG-amine (MW of 1,100; Quanta BioDesign) by cross-linking with EDC and sulfo-NHS (Pierce) as described (5) and suspended at $\sim 5 \times 10^8$ particles per milliliter in buffer A (10 min); 5 vol of fluorescent daughter beads (0.2-μm diameter, Red; Molecular Probes), which were found to bind to the magnetic beads, at $\sim 2 \times 10^9$ particles per milliliter in buffer A (5 min); 5 vol of buffer B [50 mM Tris·HCl (pH 7.9 at 23 °C), 0.1 mM EDTA, 50 mM NaCl, 10 mM $MgCl_2$, 5 mM DTT, 5 mM ATP]; and 5 vol of 0.001–10 nM reverse gyrase in buffer B. Finally, we sealed the main chamber with quick dry epoxy (Debcon) and the side chamber with silicone grease. During the infusions (at room temperature), the chamber was placed under a 5-G magnetic field to help align the magnetic beads vertically. This magnet and fluorescent beads were omitted in the plectoneme assays shown in Fig. 4. For dilution of the enzyme stock, we used nonadsorbing tips and tubes.

Microscopy. Samples were observed on an inverted microscope (IX71 or IX73; Olympus) with a 100× oil-immersion objective (UPALSAPO100X; Olympus). Fluorescent daughter beads were observed with standard epifluorescence optics consisting of a mercury lamp and a mirror unit (U-MWIG3; Olympus), and magnetic beads were illuminated with ring-type light-emitting diodes (Moritex). Images were captured with an EM-CCD camera (ADT-33B; Flovel) at 30 Hz and recorded on a hard disk with VideoSavant 4.0 software (IO Industries). Bead rotation was analyzed by tracing the centroid of a fluorescent daughter bead (6).

To control the sample temperature, we placed a copper-made custom holder (Fig. 1*B*) on a stable microscope stage (KS-O; ChuukoushaSeisakujo) and attached a tightly fitted copper jacket on the objective. For rapid temperature control, two circulating water baths set at desired temperatures were connected alternately to the water channels inside the holder and jacket. The sample temperature was monitored with a thermocouple (K type, 50-μm diameter; Ishikawa Sangyo) in the side chamber at a distance of ~5 mm from the observed area and recorded on a data logger (TC-08; Pico Technology) synchronously with the video images. When we placed another thermocouple in the main chamber, the two agreed within ±1 °C.

A neodymium cylinder magnet, with a diameter of 10 mm and height of 10 mm with a conical iron headpiece 3 mm high (Fig. 1*D*), was placed above the sample to pull the bead (7). The vertical pulling force F was calibrated by tethering the magnetic bead with 16.5-μm-long λ-phage DNA and measuring at 23 °C the amplitude of the Brownian fluctuations of the bead (8). We used a water immersion lens to estimate the bead height z from the movement of the objective needed for focusing and recorded the bead position (x, y) for 5 min at 60 frames per second at 23 °C. We estimated the tension as $F = 2k_BTz/(\delta x^2 + \delta y^2)$, where the thermal energy k_BT was taken as 4.1 pN·nm and δx^2 and δy^2 are variances of the bead position.

To control the bead orientation (Fig. 4), we used a pair of neodymium square magnets ($8 \times 8 \times 6\ \text{mm}^3$) separated by a 1-mm gap and mounted on a motor-controlled holder. Because the focus drift was appreciable at 71 °C, we included in the sample biotinylated 2-μm beads, which were tightly bound to the streptavidin-coated surface and served as a height reference. We illuminated both the magnetic and reference beads through the narrow gap between the magnets and deliberately defocused the bead image to estimate the bead height z from the diffraction pattern (9) (Fig. S3*A*). We estimated the size of the first diffraction ring by fitting its intensity distribution with a circle with a Gaussian radial profile. To convert the ring size to z, we imaged surface-stuck magnetic beads and reference beads at various focal positions. This calibration was made with the water and oil immersion objectives; for the latter, we corrected the apparent height (distance moved by the objective) for the refraction at the water/glass interface by multiplication by 1.15 = 1.52/1.33, the ratio of refractive indices of glass and water. The narrow illumination would ensure this simple correction. We measured the vertical pulling force F of the magnet pair with the λ-DNA as above and fitted the force (F) − extension (z) data with the worm-like chain model (10). The estimated persistence length and contour length at 23 °C in buffer A containing 5 mM DTT were 56.6 nm and 16.4 μm with water immersion and 56.3 nm and 16.3 μm with oil, which are in reasonable agreement. We applied the same height correction in the reverse gyrase assays using the oil-immersion objective (Fig. 4), ignoring the temperature dependence of the refractive indices. The origin of z ($z = 0$ when the bead sits on the surface) was taken close to the lowest points in the unfiltered time course for each measurement. In rare instances, a bead attached to the surface and ceased fluctuation. From these events, we estimate the precision in the z origin to be ±0.05 μm.

ATPase Activity. ATP hydrolysis by reverse gyrase was assayed as described (11). For this experiment, we prepared two essentially

complementary 147-mer oligonucleotides copied from the mid-bubble DNA except for the bubble portion. One was used as ssDNA. Annealing of the two produced 143-mer dsDNA with a 30-nt central bubble and 4-nt ss tails (Fig. S4*E*). We started an assay by incubating 10 nM reverse gyrase at 71 °C in buffer B (−ATP) without or with 100 nM DNA. The solution was capped with mineral oil to avoid evaporation. After 5 min, we started the reaction by adding ATP to the final concentration of 5 mM. At intervals (0, 5, 10, 30, 60, and 120 min), a 20-μL aliquot was drawn and quenched by ice-cold perchloric acid (final = 0.1 M). After centrifugation, the mixture was neutralized with cold NaOH and analyzed by reverse phase chromatography (ODS-100V; Tosoh) as detailed in the legend for Fig. S4.

1. Nakasu S, Kikuchi A (1985) Reverse gyrase; ATP-dependent type I topoisomerase from *Sulfolobus*. *EMBO J* 4(10):2705–2710.
2. Hsieh TS, Plank JL (2006) Reverse gyrase functions as a DNA renaturase: Annealing of complementary single-stranded circles and positive supercoiling of a bubble substrate. *J Biol Chem* 281(9):5640–5647.
3. Revyakin A, Ebright RH, Strick TR (2005) Single-molecule DNA nanomanipulation: Improved resolution through use of shorter DNA fragments. *Nat Methods* 2(2):127–138.
4. Itoh H, et al. (2004) Mechanically driven ATP synthesis by F_1-ATPase. *Nature* 427(6973):465–468.
5. Kim S, Blainey PC, Schroeder CM, Xie XS (2007) Multiplexed single-molecule assay for enzymatic activity on flow-stretched DNA. *Nat Methods* 4(5):397–399.
6. Yasuda R, Noji H, Yoshida M, Kinosita K, Jr, Itoh H (2001) Resolution of distinct rotational substeps by submillisecond kinetic analysis of F_1-ATPase. *Nature* 410(6831):898–904.
7. Harada Y, et al. (2001) Direct observation of DNA rotation during transcription by *Escherichia coli* RNA polymerase. *Nature* 409(6816):113–115.
8. Strick TR, Allemand JF, Bensimon D, Bensimon A, Croquette V (1996) The elasticity of a single supercoiled DNA molecule. *Science* 271(5257):1835–1837.
9. Gosse C, Croquette V (2002) Magnetic tweezers: Micromanipulation and force measurement at the molecular level. *Biophys J* 82(6):3314–3329.
10. Bustamante C, Marko JF, Siggia ED, Smith S (1994) Entropic elasticity of λ-phage DNA. *Science* 265(5178):1599–1600.
11. Jungblut SP, Klostermeier D (2007) Adenosine 5′-O-(3-thio)triphosphate (ATPgammaS) promotes positive supercoiling of DNA by T. maritima reverse gyrase. *J Mol Biol* 371(1):197–209.

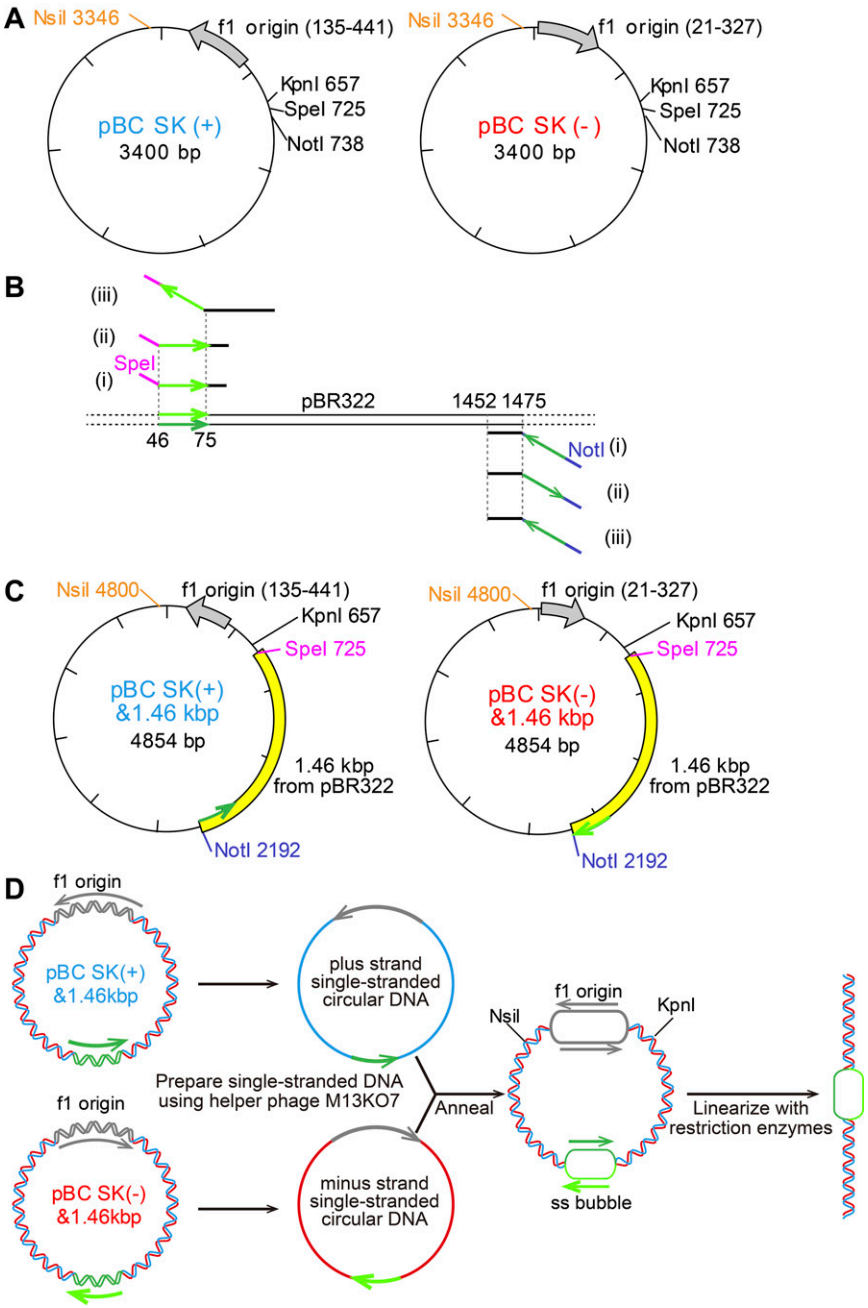

Fig. S1. Preparation of DNA substrates. The bubbled DNA substrates shown in Fig. 1*A* were prepared by annealing a complementary ssDNA pair containing a 30-nt mismatch essentially as described (1) and appending a biotinylated fragment and a digoxigenin (DIG)-labeled fragment at each end (2). (*A*) To prepare the ssDNA pair, we first introduced an NsiI site at 3,346 in pBC SK(+) and pBC SK(–) phagemid vectors (Stratagene), which contain an ssDNA replication origin (f1) in the (+) or (–) orientation. (*B*) To construct the 30-nt bubble shown in Fig. 1*A*, we prepared from pBR322 three kinds of 1.46-kbp fragments flanked by SpeI and NotI sites, using the primer pairs i–iii. The green arrows show the pBR322 sequence from 46 to 75 in this direction, with light and dark colors distinguishing the two complementary strands. (*C*) For the mid-bubble substrate, the 1.46-kbp fragments prepared by primer pairs i and ii were each introduced into pBC SK(+) and pBC SK(–), respectively, between the SpeI and NotI sites. The NotI ends of the two constructs differed in polarity (green arrows are shown for the strand that will be copied by helper phase in *D*). For the end bubble, we used primer pairs i and iii, resulting in opposite polarities on the SpeI ends. (*D*) We added helper phage M13KO7 (New England Biolabs), which is a derivative of M13 bacteriophage, to each construct to obtain ssDNA dictated by the f1 origin. The ssDNA pair (cyan and red) was annealed and linked by reverse gyrase in the presence of ADP. Finally, we digested the circular dsDNA with NsiI and KpnI to obtain a linear duplex with a bubble. For the control DNA without a bubble, we simply digested the left construct in *C*. To add a biotinylated end to the obtained linear DNA duplexes, we prepared a 1-kbp fragment with PCR using pBC SK(+) as a template (upstream from NsiI) and an equimolar mixture of biotin-labeled dUTP and nonlabeled dNTP. A 1-kb DIG-labeled end was prepared similarly from the downstream sequence from KpnI. The biotin- and DIG-labeled 1-kb ends were then ligated to the NsiI-KpnI fragment as described by Revyakin et al. (2).

1. Hsieh TS, Plank JL (2006) Reverse gyrase functions as a DNA renaturase: Annealing of complementary single-stranded circles and positive supercoiling of a bubble substrate. *J Biol Chem* 281(9):5640–5647.
2. Revyakin A, Ebright RH, Strick TR (2005) Single-molecule DNA nanomanipulation: Improved resolution through use of shorter DNA fragments. *Nat Methods* 2(2):127–138.

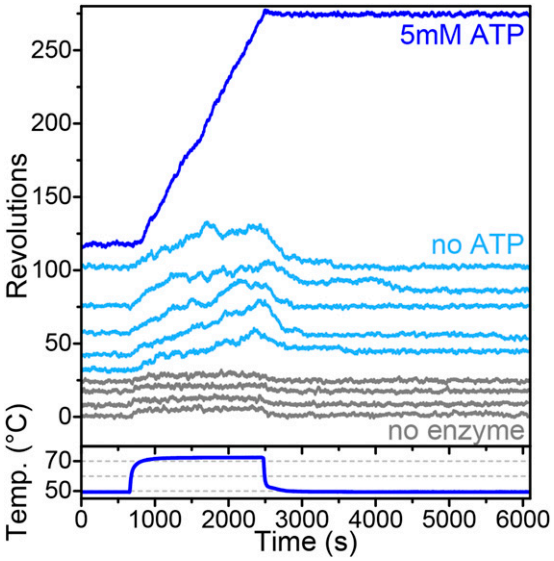

Fig. S2. DNA unwinding by binding of reverse gyrase in the absence of ATP. A long-time version of the experiments in Fig. 2*B* (*Left*) is shown. A bead tethered by the nonbubble DNA was observed under 0.5 pN of tension in the presence of 10 nM reverse gyrase. The slow rotation at 71–72 °C in the absence of ATP is reversed upon cooling to 50 °C. The interpretation is that thermal unwinding of DNA is progressively stabilized by successive binding of reverse gyrase and, upon cooling, renaturation proceeds following stochastic unbinding of reverse gyrase. At 71–72 °C, unwinding continues because already melted regions are stabilized by reverse gyrase, whereas the rest of DNA is kept relaxed by bead rotation, allowing further melting. Such unwinding cannot take place in a circular plasmid, but if the DNA is nicked, reverse gyrase can unwind the plasmid DNA in the absence of ATP (1). (*Top*) In our bead rotation assay in the presence of ATP, the bead rotated faster, as shown in this trace. This rotation must be caused by genuine overwinding activity of reverse gyrase, because the introduced turns remained after cooling.

1. Jaxel C, et al. (1989) Reverse gyrase binding to DNA alters the double helix structure and produces single-strand cleavage in the absence of ATP. *EMBO J* 8(10):3135–3139.

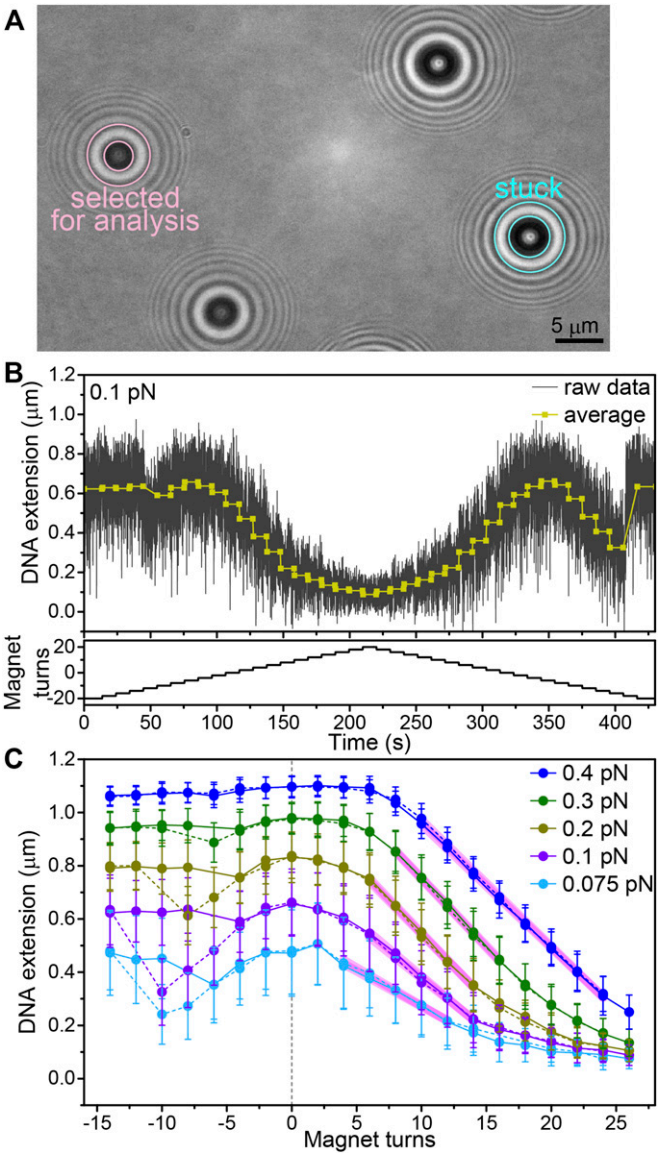

Fig. S3. Dependence of DNA extension on twist turns. (*A*) Snapshot of tethered 1-μm beads and a surface-stuck 2-μm bead. We slightly defocus the image such that diffraction rings show up. The first ring between two concentric circles is fitted with a circle with a Gaussian radial profile. The ring diameter thus estimated is converted to the bead height on the basis of separate calibration. (*B*) Partial time course of extension-rotation measurement. At each tension, we rotate a bead from −20 turns to +20 turns and back to −20 turns in steps of two turns with 10-s pause in between. The return cycle is then repeated at a different tension. The average bead height and the fluctuation amplitude (SD) during each 10-s pause are recorded. The erratic behaviors at the beginning and end of this time course are due to thermal melting and renaturation of the DNA, as explained in *C*. (*C*) DNA extension (bead height) against twist turns (*m*). Solid lines represent measurements from negative to positive turns, and dashed lines represent measurements back to negative. Error bars show SD for thermal fluctuations over 10 s. In Fig. 4*B* (*Right*), we only show the results of positive-to-negative excursions. The mid-bubble DNA at 71 °C in the absence of reverse gyrase is shown. The highest extensions are assigned to $m = 0$ (fully relaxed state). On the negative (unwinding) side, the extension tends to remain high particularly at higher tensions. This tendency is due to partial melting of underwound DNA, which requires >0.5 pN of tension at room temperature (1). At 71 °C here, DNA melts more readily and renaturation also takes place at low tensions, leading to the instability seen in *B*. Measurements interrupted by these instabilities (and by rare attachment of the bead to the glass surface) are omitted from this graph. On the positive (overwinding) side, which is related to the reverse gyrase activity, we estimate the slope of the linear portion by fitting a straight line (magenta) to the segment starting at 90% of the highest extension and ending at 30% or 0.2 μm, whichever is higher. Seven beads (8–12 slopes because not all measurements were successful) gave consistent results: 31 ± 5 nm per turn at 0.075 pN, 41 ± 3 nm per turn at 0.1 pN, 47 ± 5 nm per turn at 0.2 pN, 49 ± 3 nm per turn at 0.3 pN, and 46 ± 1 nm per turn at 0.4 pN. These average values are used for the estimations of reaction rates and required torque.

1. Strick T, Allemand JF, Bensimon D, Lavery R, Croquette V (1999) Phase coexistence in a single DNA molecule. *Physica A* 263(1-4):392–404.

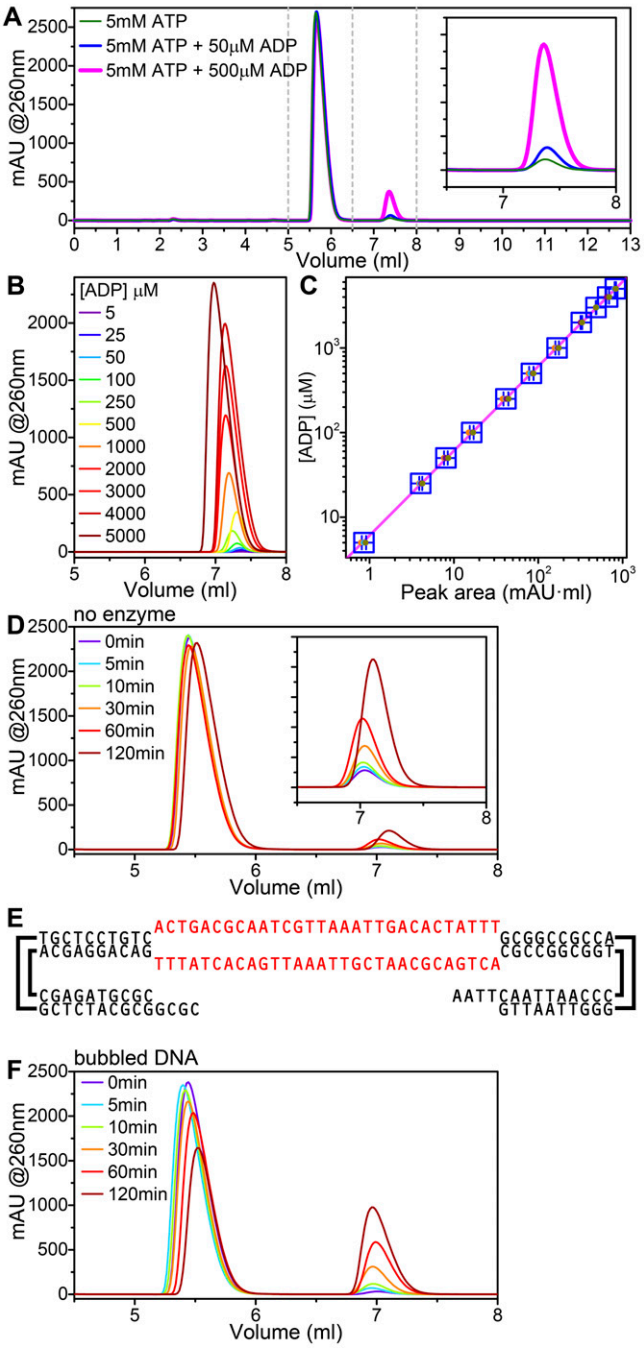

Fig. S4. ATP hydrolysis assay. (*A*) Separation of ATP and ADP by reverse phase chromatography. The ATP peak appears between 5 and 6.5 mL, and the ADP peak appears between 6.5 and 8 mL, which is magnified (*Inset*). The ATP we used contained ~1% ADP, which was corrected for in the hydrolysis assays below. mAU, milli absorbance unit. (*B* and *C*) Calibration with known concentrations of ADP. The ADP had been purified with a MonoQ 5/50 GL column (GE Healthcare), showing no trace of ATP. The peak area between 6.5 and 8 mL was used to quantify ADP. (*D*) Hydrolysis of 5 mM ATP at 71 °C in the absence of reverse gyrase. The assay was performed as described in *SI Methods*, omitting reverse gyrase. The hydrolysis rate estimated in three samples (Fig. 6) averaged 2.3 ± 0.1 μM ATP per minute per 5 mM ATP = $(4.6 \pm 0.2) \times 10^{-4}$ min^{-1} in buffer B at 71 °C, close to the literature value at 70 °C and pH 7.6 in the presence of Mg^{2+} of 3.82×10^{-4} min^{-1} (1). We did not detect an ADP increase over 1 h of incubation at room temperature. (*E*) Bubbled DNA used in the ATPase assay. The bubble here is a combination of one bubble strand in Fig. 1*A* and its reversed sequence. (*F*) Hydrolysis of 5 mM ATP by 10 nM reverse gyrase in the presence of 100 nM bubbled DNA. The assay at 71 °C was performed as in *SI Methods*. Three samples gave an average hydrolysis rate of 14.3 ± 1.6 μM·min^{-1}, from which the rate in the absence of the enzyme in *D* was subtracted to give the ATPase activity as 20 ± 3 s^{-1} (Fig. 6).

1. Ramirez F, Marecek JF, Szamosi J (1980) Magnesium and calcium ion effects on hydrolysis rates of adenosine 5′-triphosphate. *J Org Chem* 45(23):4748–4752.

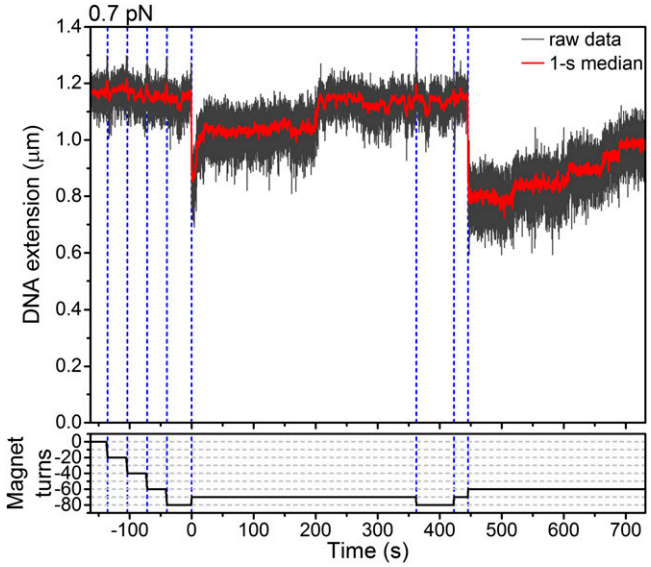

Fig. S5. Relaxation of positive supercoils at high tension. With the experimental setup in Fig. 4, we applied 0.7 pN of tension to the DNA in the presence of 1 nM reverse gyrase. Under this high tension, unwinding maneuvers by 20 turns with magnets did not change the bead height (before 0 s). Presumably, reverse gyrase relaxed the introduced negative torsions and, by time 0, wound the DNA to a slightly overwound state. Thus, only 10 positive turns with magnets at 0 s brought down the bead appreciably. The downward movement must be due to the introduction by magnets of plectonemes (positive supercoils), which required ~8 pN·nm of torque under 0.7 pN of tension. This high torsional stress exceeding Γ_c of ~5 pN·nm let reverse gyrase work in reverse: The bead rose to the original height in two steps, showing relaxation of positive supercoils by reverse gyrase. From ~360 s, we repeated similar maneuvers. In this trial, the first positive 10 turns at ~420 s failed to sink the bead, indicating that reverse gyrase had not yet overwound the DNA sufficiently, but the second 10 turns at ~445 s brought the bead down. Thereafter the bead again rose toward the original height, indicating relaxation of positive supercoils. We could repeat such maneuvers several times on the same bead, showing that the rise of the bead was not due to DNA nicking. The relaxation kinetics varied from trial to trial and from bead to bead.

Movie S1. Rotation of a fluorescent daughter bead in response to DNA overwinding by reverse gyrase. The portion between 1,722 and 1,823 s of the red curve in Fig. 2*B* is shown. The experiment was with 10 nM reverse gyrase and mid-bubble DNA at 71 °C. The image size is 3.6 × 3.6 μm^2.

Movie S1